Analytical Methods

Accepted Manuscript

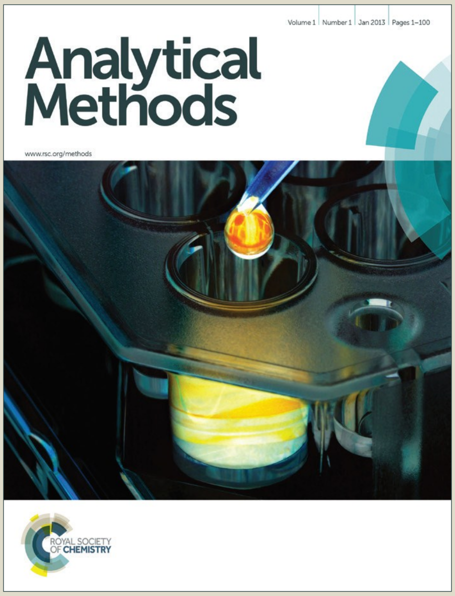

ROYAL SOCIETY OF CHEMISTRY

www.rsc.org/methods

Electrical conductivity, isothermal stability and amine sensing studies of synthetic *p*-toluenesulfonic acid doped Poly-*o*-toluidine/multi-walled carbon nanotubes/ Sn(IV)tungstate composite ion exchanger

Asif Ali Khan*, Shakeeba Shaheen

Abstract

Electrically conductive *p*-toluenesulfonic acid (*p*TSA) doped Poly-*o*-toluidine (POT) composite were prepared with multi-walled carbon nanotubes (MWCNTs) and Sn(IV)tungstate (ST) by insitu oxidative polymerization. The *p*TSA doped POT, POT/MWCNTs and POT/MWCNTs/ST composites were characterized by Fourier transform infra-red spectroscopy (FTIR), X-ray diffraction (XRD), Scanning electron microscopy (SEM), Transmission electron microscopy (TEM), UV–visible spectra and thermogravimetric analysis (TGA). The TGA studies revealed that POT/MWCNTs/ST composite was thermally more stable in comparison to pure polymer and POT/MWCNTs. The electrical conductivity behavior of POT/MWCNTs was observed better than pure POT and POT/MWCNTs/ST. Ammonia and amines vapour sensing studies of POT/MWCNTs/ST composite ion exchangers have shown improved performance.

Keywords: MWCNTs; Poly-*o*-toluidine; Electrical conductivity; Thermal stability; Ammonia Sensing

1. Introduction

The serendipitous discovery of conducting polyacetylene film on doping with iodine is a classic episode in the history of invention [1]**.** Later, many other polymers were found to be conductive as the research in this field grew by leaps and bounds [2-6]**.** Conducting polymers are a unique class of materials exhibiting electrical and optical properties of metals or semiconductors. These materials have unique potential for use in various devices due to their architectural diversity and flexibility, inexpensiveness, and ease of synthesis [7-8]**.**

Amongst the various conducting polymers, polyaniline (Pani) has been a candidate of enormous research due to its exciting properties, such as low cost of its monomers, high stability, ease of synthesis, good control of its conducting and non conducting states by simple acid base chemistry, etc [9-11]**.** However, apart from Pani, nanocomposites of its derivatives such as poly(o-anisidine), poly(o-toluidine), polypyrrole, polythiophene have also been investigated for electrical conductivity and sensing properties. These conductive polymers have better chemical properties of solubility with respect to normal Pani and its capacity is preserved in sensing analysis [12-15]. Such nanocomposites have shown good performance in low current experiments. Recently, scientists have found that the substitution on the phenyl ring enhances the solubility of Pani as it probably opens the chain structure, thereby giving greater chance for the solvent to solubilise it [16-17]**.**

The use of derivatives of Pani such as Poly-*o*-toluidine (POT), by alkyl substitution on the phenyl moiety of Pani has shown a new opening, as the resulting polymer or its derivatives after modification are not only conducting but they can also be processed into a variety of forms with relatively more ease than Pani. Since the nanoform of this polymer could offer exciting properties or enhanced performance, composites of conducting polymer such as POT has gained enormous interest in the recent years. In order to achieve the advantageous properties arising due to nanoscale dimensions, carbon nanotubes based conducting polymer composites have gained much attention during the past few years due to the synergism between the constituents. It is well known that the strong interaction between the POT aromatic ring and graphitic structures of carbon nanotubes would be a great benefit to the charge-transfer interaction between the two components with newer set of properties, and may find potential application for use in nanotechnologies and devices [18-21]. However, it is also cited in literature that carbon nanotubes contain metal impurities which are responsible for electrocatalysis or electroanalysis seen at some nano tube modified electrodes [22-23]. The presence of CNT during the polymerization of polymer induces the formation of a more planar conformation of polymer which acts as a coating layer for the carbon nanotubes and leads to favourable interaction between the constituents. The polymer coated CNT are aligned into bundles and form a three-dimensional network in the composites. These findings have important consequences for many applications, especially in the development of polymer composite [24-31]**.** The polymeric composite materials have shown better ion exchange behaviour as well as good electrical response [12-13, 15]**.**

In the present work, our aim is to prepare composite materials with better ion exchange as well as electrical properties for analytical and electroanalytical studies. Thus we have prepared *p*TSA doped POT, MWCNTs and ST based composite ion exchanger by simple insitu oxidative polymerization of POT in the presence of MWCNTs and ST ion exchangers. The POT, POT/MWCNTs and POT/MWCNTs/ST composite ion exchangers have shown good electrical response for amine sensing studies and better ion exchange capacity respectively.

2. Experimental

2.1. Chemicals, reagents and instruments

Double distilled *o*-toluidine, HCl (35%) from E-Merck (India Ltd.) and MWCNTs from Iljin Nano Tech, Seoul, Korea (diameter ~ 10-20 nm and average length ~ 20 μm) were used. Ammonium persulphate (Qualigens, 98%) CTAB (Cetyl trimethylammonium bromide), methanol from CDH (India Ltd. 98%), *p*-toluenesulfonic acid (*p*TSA) from Qualigens (AR grade 98%), and Demineralised water (DMW) were used in the experimental work. All other reagents and chemicals were of analytical grade.

Following instruments used: Fourier transform infra-red (FTIR) spectrophotometer (Perkin-Elmer, USA, model Spectrum-BX, range 4000-400 nm), Scanning electron microscope (SEM) and Transmission electron microscopy (TEM) (LEO 435–VF), thermo-gravimetric analysis (TGA) using thermal analyzer-V2.2A DuPont 9900 in nitrogen atmosphere and Rigaku X-Ray powder diffractometer (XRD) with Cu anode (Kα λ=1.54186 A°) using a PW, 1148/89 based diffractometer with Cu Kα radiations, Elmasonic sonicater (Frequency 37kHz), UV-Visible spectra of Perkin Elmer (Pyris Dimond) spectrophotometer in the range of 190-1100nm. A four point probe electrical conductivity measuring instrument (Scientific Equipment Roorkee, India) was used for measuring DC electrical conductivity and sensing studies.

2.2. Synthesis of POT, POT/MWCNTs and POT/MWCNTs/ST composite ion exchanger

In a typical process, CTAB was added to 300 ml of 1M HCl by stirring, which was followed by the addition of monomer *o*-toluidine. MWCNTs in HCl was ultrasonicated for 1hour and was added to the above mixture which was put under vigorous stirring. The solution of oxidant ammonium per sulphate was added later, which changed the colour of the solution from pink to green, indicating the polymerization process. The whole system was put under vigorous stirring for 24 hours after that the sample was filtered, washed with DMW and later with excess of methanol until the filtrate becomes colourless. The composite (POT/MWCNTs) was later doped with *p*TSA solution made in EDTA to render its conductivity. Pure POT was prepared similarly in the absence of MWCNTs. In the case of POT/ MWCNTs/ST, the inorganic Sn(IV)tungstate (prepared by mixing 200 ml of 0.1M stannic chloride made in 1M HCl with 50 ml of 0.1M sodium tungstate in DMW) [32] was added after the addition of MWCNTs.

2.3. Studies

2.3.1. Composition

The properties, particle size, morphology, thermal stability and the functional groups present in the prepared POT, POT/MWCNTs and POT/MWCNTs/ST composite ion exchanger materials were characterized by using SEM (Scanning electron microscopy), energy dispersive

X-ray (EDX) (LEO 435-VF), TEM (Transmission electron microscopy), XRD (X-ray diffraction), FTIR (Fourier transform infrared), TGA (Thermogravimetric analysis) techniques and UV-Visible spectra.

2.3.2. Ion exchange studies

The ion exchange capacity (IEC), which is generally taken as a measure of the hydrogen ion (H^+) liberated by neutral salt to flow through the composite was determined by standard column process reported as earlier [33],

2.3.3. Electrical conductivity studies

The electrical conductivity was measured using four point probe. The selected samples of composite were dried at 40–50 °C in an oven for 24 h. The pellets of the composite materials

(500 mg) were made at room temperature with the help of a hydraulic pressure at 25 kN applied for 10 min. The conductivity (σ) was calculated using the following equation [34];

$$\sigma = [\ln 2(2S/W)] / [2\pi S(V/I)] \qquad (1)$$

Where I, V, W and S are the current (A), voltage (V), thickness of the film (cm) and probe spacing (cm) respectively and σ is the DC electrical conductivity (S/cm).

The isothermal stability of the composite materials in terms of retention of DC electrical conductivity was carried out at 50, 70, 90, 110 and 130 °C in an air oven and the conductivity measurements were recorded at every after 10 min interval of time.

2.3.4. Sensing measurements studies

The vapour sensing measurements of 0.5M aqueous ammonia and methyl amine (i.e. NH_3 and $-CH_2NH_2$) were done by monitoring the resistivity of the composites using four point probe in a glass chamber. The sample to be tested as sensor was placed on the base plate of four point probe arrangement and the probe was allowed to rest in the middle of the sample. The vapour sensitivities were recorded by their electrical responses, the current voltage characteristic gave the resistivity of the samples [35]. The Schematic diagram of sensor set-up for ammonia and amine sensing based on four point probe electrical conductivity measuring instrument is shown in **Figure 1.**

3. Result and Discussion

3.1. Synthesis of POT, POT/MWCNTs and POT/MWCNTs/ST composite ion exchangers

POT, POT/ MWCNTs and POT/MWCNTs/ST composite ion exchangers were prepared by simple insitu oxidative polymerization of o-toluidine in the presence of MWCNTs and Sn(IV)tungstate under different conditions (**Table 1**). The POT/MWCNTs /ST composite ion exchanger possessed better Na^+ ion exchange capacity (IEC) (1.25 $meqg^{-1}$) as compared to POT/MWCNTs composite (0.90 $meqg^{-1}$) and pure POT (1.05 $meqg^{-1}$). The schematic representation of the formation of POT, POT/MWCNTs and POT/MWCNTs/ST composites ion exchanger are shown in **Scheme. 1.**

From EDX result the percentage composition of the elements present in the POT/MWCNTs/ST composite ion-exchange material for C, N, O, Sn and W are 78.69%, 1.44%, 6.87%, 8.20% and 4.80% respectively.

FTIR spectra of POT, POT/MWCNTs and POT/MWCNTs/ST composite ion exchangers are presented in **Figure 2**. For POT, the absorption band at around 3017 cm^{-1} corresponds to N–H stretching mode of secondary amine. The two bands at around 1485 and 1598 cm^{-1} are assigned to the stretching vibration of the benzenoid and quinoid ring respectively. The characteristic bands at about 3017 cm^{-1} can be assigned to the stretching vibration of the methyl ($–CH_3$) group, while the band at 1386 cm^{-1} is due to the symmetric deformation of methyl group. The bands at 1314 and 1213 cm^{-1} can be assigned to the C–N vibration. The three bands appearing at 1008, 873 and 812 cm^{-1} were attributed to an out-of-plane C–H vibration, 1,2,4-substitution in the benzenoid rings, and in-plane C–H vibration of quinoid rings respectively. These data are similar to the spectra of POT salts, which confirmed that the obtained sample is in its doped phase [36]**.** The FTIR spectra of POT/MWCNTs composite are almost identical to that of POT, indicating that *o*-toluidine was polymerized on the surface of MWCNTs and no chemical interaction has taken place. In the FTIR spectra of POT/MWCNTs/ST composite, the peak at 2923 cm^{-1} indicates stretching frequency of C≡N group and peak at 1600 cm^{-1} represents the free water molecule (water of crystallization) bending bands. The two peaks at 1487cm^{-1} and at 1117 cm^{-1} represents C-H vibration and phosphate group. Other two peaks assemblies at 814 and 566 cm^{-1} represent Sn-O groups [37].

The XRD patterns (**Figure 3)** of POT and POT/MWCNTs showed similarity in crystalline regions, indicating that MWCNTs does not affect the crystallinity of the POT. Since both materials are crystalline in nature. However the peaks at 2θ = 20°-50° in the case of POT/MWCNTs/ST showed some amorphosity which may be due to some sort of interaction of polymer with the inorganic precipitate Sn(IV) tungstate, since Sn(IV) tungstate is an amorphous material [38].

The TGA curves in **Figure 4** shows distinct weight losses of POT, POT/MWCNTs and POT/MWCNTs/ST. In TGA curve of POT shows slow degradation of mass starts from 50 °C and about 10% weight is lost upto 200 °C which may be due to removal of water molecules. From 200 °C on words material starts to decompose and upto 900 °C about 60% weight is lost. The TGA curve of POT/MWCNTs composite shows the weight loss upto 5% at 50-200 ºC due to the removal of external water molecules, however this material retain ~80% of mass after heating upto 300 ºC and further decomposition of the material ~15% was also observed upto 900 ºC. In the case of POT/MWCNTs/ST, the degradation starts from 50 °C as in the case of above two materials, first the water molecules were removed then ~90% degradation of this material at 1000 ºC is quite clear from the figure. Thus it is evident from the results of TGA that POT/MWCNTs/ST ion-exchange nanocomposite is thermally more stable than POT and POT/MWCNTs composite.

The surface morphology of *p*TSA doped POT, POT/MWCNTs and POT/MWCNTs/ST composites were studied by SEM as shown in **Figure 5**. The granular structures are seen in the SEM picture of POT. These granular structures can also be seen in the SEM picture of POT/MWCNTs and POT/MWCNTs/ST. It may be due to some o-toluidine monomers have polymerized on the surface of MWCNTs templates and the remaining amount of o-toluidine monomer have polymerized into granular structures.

Figure 6 shows TEM micrograph of *p*TSA doped POT/MWCNTs/ST composite, it is clear from the figure that the individual fibrous phases of POT/MWCNTs/ST containing MWCNTs. The tubular structure of MWCNTs in POT/MECNTs/ST composite is also quite evident in figure. However, the coating of the fibrous phase is not really homogeneous and composed of more “block-like” structures.

The UV–visible spectra of the POT, POT/MWCNTs and POT/MWCNTs/ST in 1M *N*-methyl-2-pyrolidone (NMP) solutions are presented in **Figure 7**. Due to deprotonation effects of NMP, the spectra are similar with that of emeraldine base of POT. The major peak observed at about 304 nm is assigned to the excitation of the benzene and quinoid segments on the polyemeraldine. The absorption peak at about 304 nm can also be ascribed π to π^* transition of the benzenoid rings, which is attributed to π^* and π–polaron transition. The sharp peak at 235nm is being due to presence of NMP [39] in all samples.

3.2. Electrical conductivity Studies

It is quite evident from the result that the conductivity increases on addition of MWCNTs to POT, however a decrease in IEC was observed. On addition of Sn(IV)tungstate in the sample POT/MWCNTs, the IEC was increased but again conductivity decreased. The increase in conductivity can be well understood from the percolative path in which the concentration of conducting particles increase, showing that the conductivity depends significantly on the carrier transport through the conducting fillers [40]. In the similar manner on addition of Sn(IV)tungstate, the IEC increased due to presence of more exchanging sites. It is also clear from the results that as MWCNTs was added to POT, some exchangeable sites were affected by conducting fillers. The electrical conductivity of the composite was also measured with increasing temperatures from 40-150 °C as shown in (**Figure 8**). There was no significant change in conductivity in the case of POT and POT/MWCNTs/ST however in the case of POT/MWCNTs, increase of conductivity with rise in temperature was observed, indicating its conduction in the absence of Sn(IV)tungstate.

It is clear from **Figure 9,** that MWCNTs has a major effect on the initial electrical conductivities of POT/MWCNTs and POT/MWCNTs/ST composite ion exchangers. The results showed that the electrical conductivity of POT/ MWCNTs composite is higher than that of POT and POT/MWCNTs/ST composite. Since POT and POT/MWCNTs is good conductor, it may be attributed to the additional and synergistic effect of both the constituents, resulting in increased electrical conductivity. MWCNTs have the ability to form efficient network for charge transport [41]. But the electrical conductivity of POT/ MWCNTs/ST is very low compared to POT and POT/MWCNTs, because of mixing of nonconductive part of Sn(IV)tungstate.

3.3. Stability in terms of DC electrical conductivity retention

The isothermal stability of the composite material in terms of DC electrical conductivity retention was carried out at 50, 70, 90, 110 and 130 °C in an air oven. The electrical conductivity measurements were done five times after an interval of 10 min at a particular temperature. The electrical conductivity measured with respect to time is presented in **Figure 10(a-c**). It was observed that all the composite materials followed Arrhenius equation [34] for the temperature dependence of the electrical conductivity from 50-90 °C and after that a deviation in electrical conductivity was observed, it may be due to the loss of dopant and degradation of materials. The stability of POT, POT/MWCNTs and POT/MWCNTs/ST composite ion exchangers in terms of DC electrical conductivity retention was found to be fairly good as studied by isothermal technique. The POT, POT/MWCNTs and POT/MWCNTs/ST composite ion exchangers can be used in electrical and electronic applications below 90 °C under ambient conditions.

3.4. Ammonia and amine sensing characteristics of POT, POT/MWCNTs and POT/MWCNTs/ST composite ion exchangers

The ammonia and amine sensing performance of POT, POT/MWCNTs and POT/MWCNTs/ST composite ion exchangers was studied by measuring resistivity changes on exposure to ammonia and methyl amine (-NH_3 and -CH_2NH_2) vapours using laboratory made assembly using four point probe electrical conductivity device. The remarkable changes in the resistivity of the composite ion exchanger on exposure to 0.5M of aqueous -NH_3 and -CH_2NH_2 solutions with vapour concentration 3.53% and 3.24% respectively of their original solutions at room temperature as a function of time (**Figure 11 (I & II)**). The POT/MWCNTs composite showed a relatively fast sensing response towards 0.5M -CH_2NH_2 as compared to the response of POT and POT/MWCNTs/ST, however as far as ammonia vapours are concerned POT/MWCNTs/ST composite ion exchange material showed better sensing response. It may be due to interaction of ammonia with H^+ (counter ion) present in the exchangeable sites of composite ion exchanger. The resistivity can be recovered on flushing with the ambient air. The response and recovery time of the POT, POT/MWCNTs and POT/MWCNTs/ST sensors were around 5 and 20s for 0.5M aqueous NH_3 and -CH_2NH_2 vapours respectively. The reversible sensing responses of 0.5M NH_3 and CH_2NH_2 vapours on polymer and composites were also investigated and were found to be highly reversible during the test of cyclic measurements. Again the vapours sensing responses were studied on POT, POT/MWCNTs and POT/MWCNTs/ST for 0.5M concentration of NH_3 and -CH_2NH_2 vapours showed a poor performance and took a long time to regain the resistivity value near to the original one. This poor response in resistivity value might be due to insufficient conductivity sites available in the composite for NH_3 and -CH_2NH_2 vapours moiety to form the complex structure necessary for obtaining the response behaviour. The extent of reversibility of the sensor was examined by successive several cyclic measurements using

0.5M concentrations of NH_3 and CH_2NH_2. From the Relative Standard Deviation (RSD) (%) it can be inference that the sensor had worked best for POT/MWCNTs composite for 0.5M concentration and at this concentration slight irreversibility was observed which might be due to the electrical compensation of the polymer backbone by NH_3 and -CH_2NH_2. On comparison of the response time, recovery time and electrical conductivity of the proposed POT/MWCNTs/ST composite ion exchanger for NH_3 and -CH_2NH_2 vapours were found better than other reported materials **[36]**. Therefore, it would be meaningful to obtain a new kind of materials with good - NH_3 and CH_2NH_2 sensing via simple preparation method.

3.5. Sensing Mechanism

The ammonia interacts with emeraldine salt of POT/MWCNTs/ST composite ion exchangers through its lone pair of electrons. As soon as this interaction takes place, the intensity of positive charge on nitrogen is decreased, leading to decrease in the mobility of charge carriers hence a decrease in electrical conductivity observed. The interaction is electrostatic in nature and due to the small magnitude of charge on both atoms the interaction is very weak, which reverses under ambient conditions and the conductivity is restored. A slight acid base neutralization also takes place due to the interaction of H^+ ion present in matrix of ion exchange material (POT/MWCNTs/ST), hence leading to decrease in conductivity after each cycle.

The interaction of methyl amine is stronger due to its three alpha hydrogen which leads to more intensity of negative charge on nitrogen hence it interacts more strongly with positive centre of imine nitrogen in comparison to ammonia. The mechanistic representation of the electrical compensation of *p*TSA doped POT/MWCNTs/ST in present research is given in **Scheme 2.**

4. Conclusion

In the present work, *p*TSA doped POT, POT/MWCNTs and POT/ MWCNTs/ST composite ion exchangers were synthesized and characterized by using different instrumental techniques such as TEM, SEM, XRD, TGA, UV-Visible and FTIR. The results of the studies reveal that the polymerization of POT has been successfully achieved on the surface of the MWCNTs and Sn(IV)tungstate. This indicates the formation of a new composite ion exchange material having good ion exchange properties. The results showed that the electrical conductivity of POT/MWCNTs composite is higher than that of POT and POT/MWCNTs/ST composite since due to the presence of carbon nanotubes. The sensing behaviours of POT/MWCNTs/ST (ion exchange composite) for 0.5M aqueous NH_3 vapour is better than that of POT and POT/ MWCNTs composite, due to the presence of more exchangeable sites in the composite ion exchanger, however there is no significant sensing response for $–CH_2NH_2$ on composite ion exchanger.

Acknowledgments

Authors are thankful to the Department of Applied Chemistry for providing the research facilities and also thankful to University Grant Commission, Government of India [42-336/2013 (SR)] for financial support.

Notes and References

Analytical and Polymer Research Laboratory, Department of Applied Chemistry, F/O Engineering and Technology, Aligarh Muslim University Aligarh 202002, India.

***Corresponding Author: Tel.** +91-571-2720323. **Fax** +91-571-270-1260

Email addresses: asifalikhan42003@yahoo.com, shakeebashaheen@ymail.com

1. H. Shirakawa, E. J. Louis, A. G. MacDiarmid, C. K. Chiang and A. Heeger, *J. Chem. Commun.,* 1977, 16, 578.

2. L. Wang, Q. Feng, X. Wang, M. Pei and G. Zhang, New J. Chem., 2012, 36, 1897.

3. J. P. Pouget, M. E. Jozefowicz, A. J. Epstein, X. Tang and A. G. MacDiarmid, *Macromolecules.,* 1991, 24, 779.

4. J. Stejskal, *Pure Appl. Chem.,* 2002, 74, 857.

5. E. Ekinci, *Polymer Bulletin.,* 1999, 42, 693.

6. H. John, M. Rinku, K. Thomas, T. Mathew and R. Joseph, *J. Appl. Polymer. Sci.,* 2004, 92, 592.

7. N. Hundt, K. Palaniappan, P. Sista, W. M. John, J. Hao, H. Nguyen, E. Stein, C. B. Michael, E. G. Bruce and C. S. Mihaela, *Polym. Chem.,* 2010, 1, 1624.

8. A. Gök, M. Omastová and A. G. Yavuz, *Synthetic Metals.,* 2007, 157, 23.

9. M. O. Ansari and F. Mohammad, *Sensor. Actuator. B: Chem.,* 2011, 157, 122.

10. M. O. Ansari and F. Mohammad, *Compos. Part B- Eng.,* 2012, 43, 3541.

11. A. D. Price, C. Vivian, K. Jennifer, X. Zhang and E. H. Naguib, *Synthetic Metals.,* 2010, 160, 1832.

12. A. A. Khan and A. Khan, *Materials Sci. Eng. B.,* 2009, **158**, 92.

13. A. A. Khan and U. Baig, *Solid State Sci.,* 2013, **15**, 47.

14. S. Pirsa and N. Alizadeh, *Sensors and Actuators B: Chemical,* 2010, **147**, 461.

15. A. A. Khan and U. Baig, *Sensors and Actuators B: Chemical,* 2013, **177**, 1089.

16. C. H. Hsieh, A. H. Lee, C. D. Liu, J. L. Han, K. H. Hsieh and S. N. Lee, *AIP Advances.,* 2012, **2,** 012127.

17. G. R. Yerawar, *Der Pharma Chemica.,* 2012, **4,** 1288.

18. D. Aussawasathien, S. Sahasithiwat and L. Menbangpung, *Synthetic Metals.,* 2008, **158,** 259.

19. K. Y. Chen, M. X. Sun, L. C. Chao Li, F. Xu and Q. S. Xiao, Adv. *Mater. Resear.,* 2011, **249,** 295.

20. N. A. Kiselev, J. Sloan, D. N. Zakharov, E. F. Kukovitskii, J. I. Hutchison and J. Hammer, *Carbon.,* 1998, **36**, 1149.

21. E. T. Thostenson, Z. F. Ren and T. W. Chou, *Compos. Sci. Technol.,* 2001, **61**, 1899.

22. B. M. Christopher, G. W. Gregory, G. C. Richard, S. Lidong and L. H. G. Malcolm*, Sens. Actuator. B,* 2008, **132,** 356.

23. B. Sÿljukic´, C. E. Banks and R. G. Compton, *Nano Lett.,* 2006, **6,** 1556.

24. S.M. Hosseini, F. Jeddi, M. Nemati, S.S. Madaeni and A.R. Moghadassi, *Desalination*, 2014, **341** 107.

25. A. Zendehnam, S. Mokhtari, S.M. Hosseini and M. Rabieyan, *Desalination,* 2014, **347**, 86.

26. T. A. Ali and G. G. Mohamed, *Sensors and Actuators B: Chemical*, 2014, **202**, 699.

27. M. Boota, K. B. Hatzell, M. Beidaghi, C. R. Dennison, E. C. Kumbur and Y. Gogotsi, *J. Electrochem. Soc.,* 2014, **161**, A1078.

28. G. Pognon, T. Brousse and D. Bélanger, *Carbon*, 2011, **49**, 1340.

29. C. Zhang, K. B. Hatzel, M. Boota, B. Dyatkin, M. Beidaghi, D. Long, W. Qiao, E. C. Kumbur and Y. Gogotsi, *Carbon*, 2014,**77**, 155.

30. M.O. Ansari, S. P. Ansari, S. K. Yadav, T. Anwer, M.H. Cho and F. Mohammad, *J. ind. eng. chem.,* 2014, **20**, 2010.

31. M.O. Ansari, S.K. Yadav, J.W. Cho and F. Mohammad, *Compos. part B-eng.,* **47**, 2013, 155.

32. A. A. Khan, S. Shaheen and U. Habiba, *J. Advance. resear.,* 2012, **3**, 269.

33. A. A. Khan and S. Shaheen, *Compos: Part B,* 2013, **44**, 692.

34. M. O. Ansari, S. A. Ansari, I. Amal, J. Lee and M. H. Cho, *Chem. Eng. J.,* 2013, **242,** 155,

35. A. A. Khan and M. Khalid, *J. Appl. Polym. Sci.,* 2010, **3,** 1601.

36. S. Ding, X. Lu, J. Zheng and W. Zhang, *Mater. Scie. Eng. B.,* 2006, **135,** 10.

37. A. A. Khan and S. Shaheen, *Solid State Sci.,* 2013, **16**, 158.

38. H. Patel, A. Parikh and U. Chudasama, *Bull. Mater. Sci.,* 2005, **28**, 137.

39. J. A. Shea, S. C. Cook, W. F. Shamrock and J. Segretario, *J. Chromatographic Sci*., 1998, **36,** 187.

40. A. A. Khan and U. Baig, *Sens. Actuat. B.,* 2013, **177**, 1089.

41. Z. Z. Zhu, Z. Wang and H. L. Li, *Appl. Surf. Sci.,* 2008, **254**, 2934.

Table 1 Conditions of preparation and IEC of POT, POT/MWCNTs and POT/MWCNTs/ ST composite ion exchanger

S. No	o-toluidine (mL)	Oxidant[*] (g)	MWCNT (g)	CTAB (g)	*p*TSA[**]	DC electrical conductivity (S/cm)	I.E.C. ($meqg^{-1}$)
POT	5	5.4	0.0	17	8.8	1.78	1.05
POT/MWCNTs	5	5.4	0.5	17	8.8	4.34	0.90
POT/MWCNTs/ST	5	5.4	0.5	17	8.8	0.2	1.25

[*] Oxidant solution was prepared by dissolving $(NH_4)_2S_2O_8$in 200 mL of 1M HCl

[**] *p*TSA solution was made by dissolving *p*TSA in 500 mL of EDTA

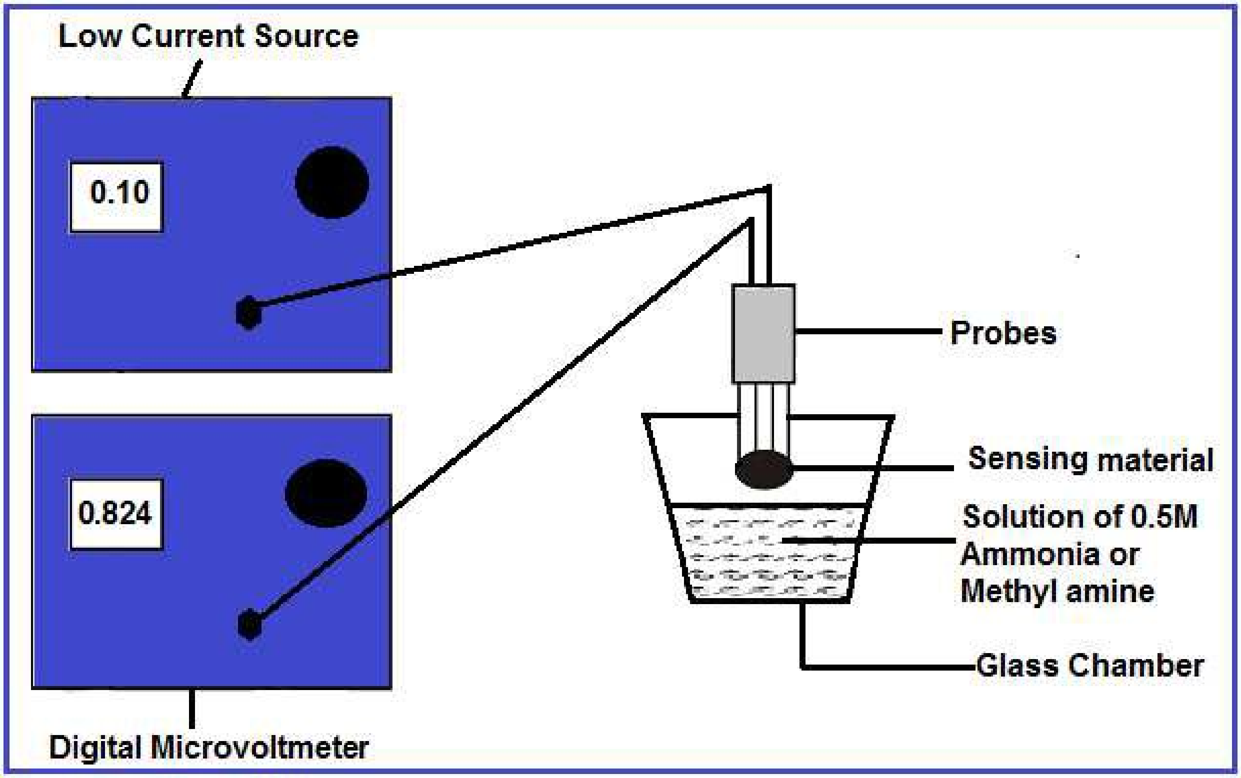

Figure 1. Schematic diagram of sensor set-up for ammonia and amine sensing based four point probe electrical conductivity measuring instrument.

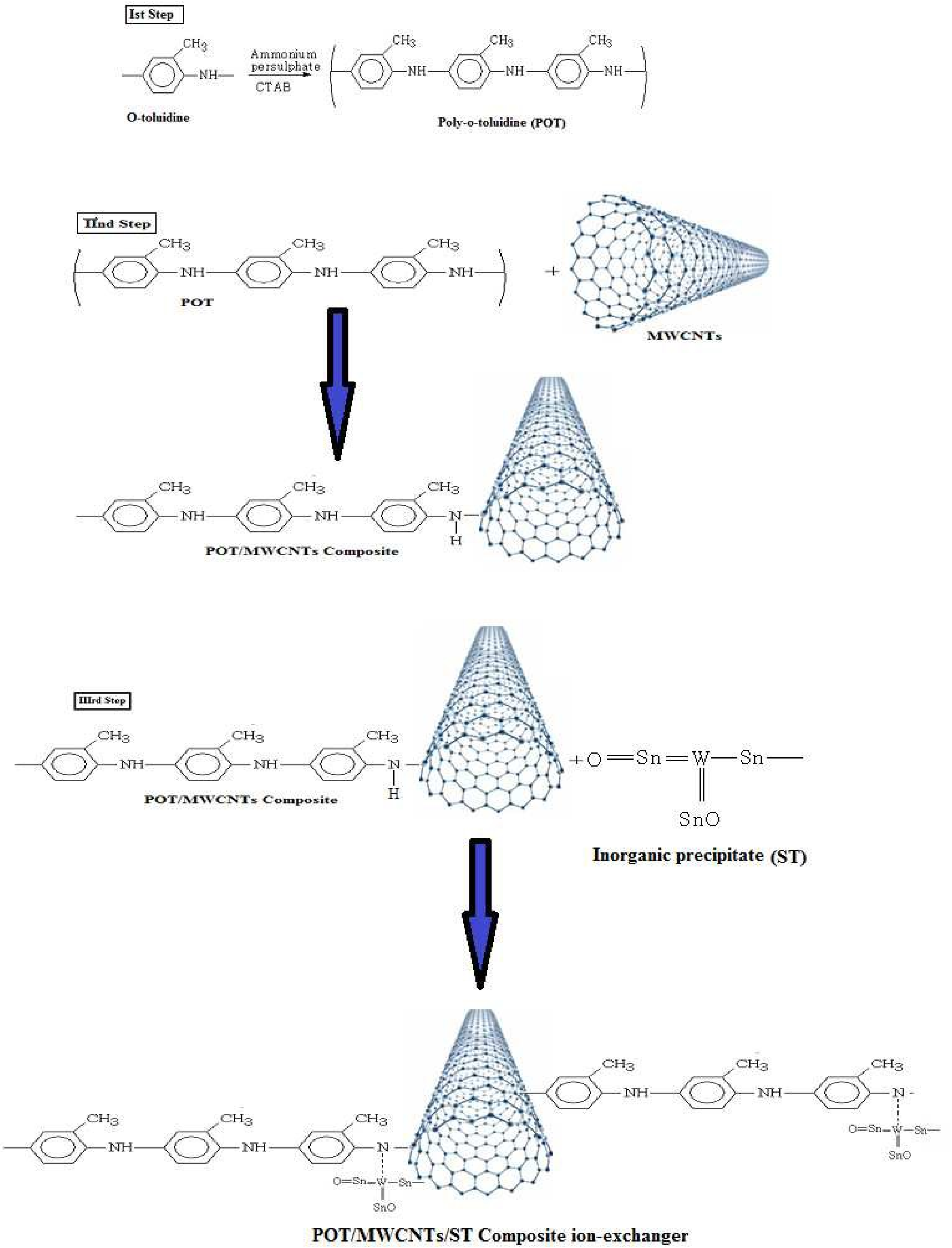

Scheme 1. The schematic representation of the formation of POT, POT/ MWCNTs and POT/ MWCNTs/ST composites ion exchanger

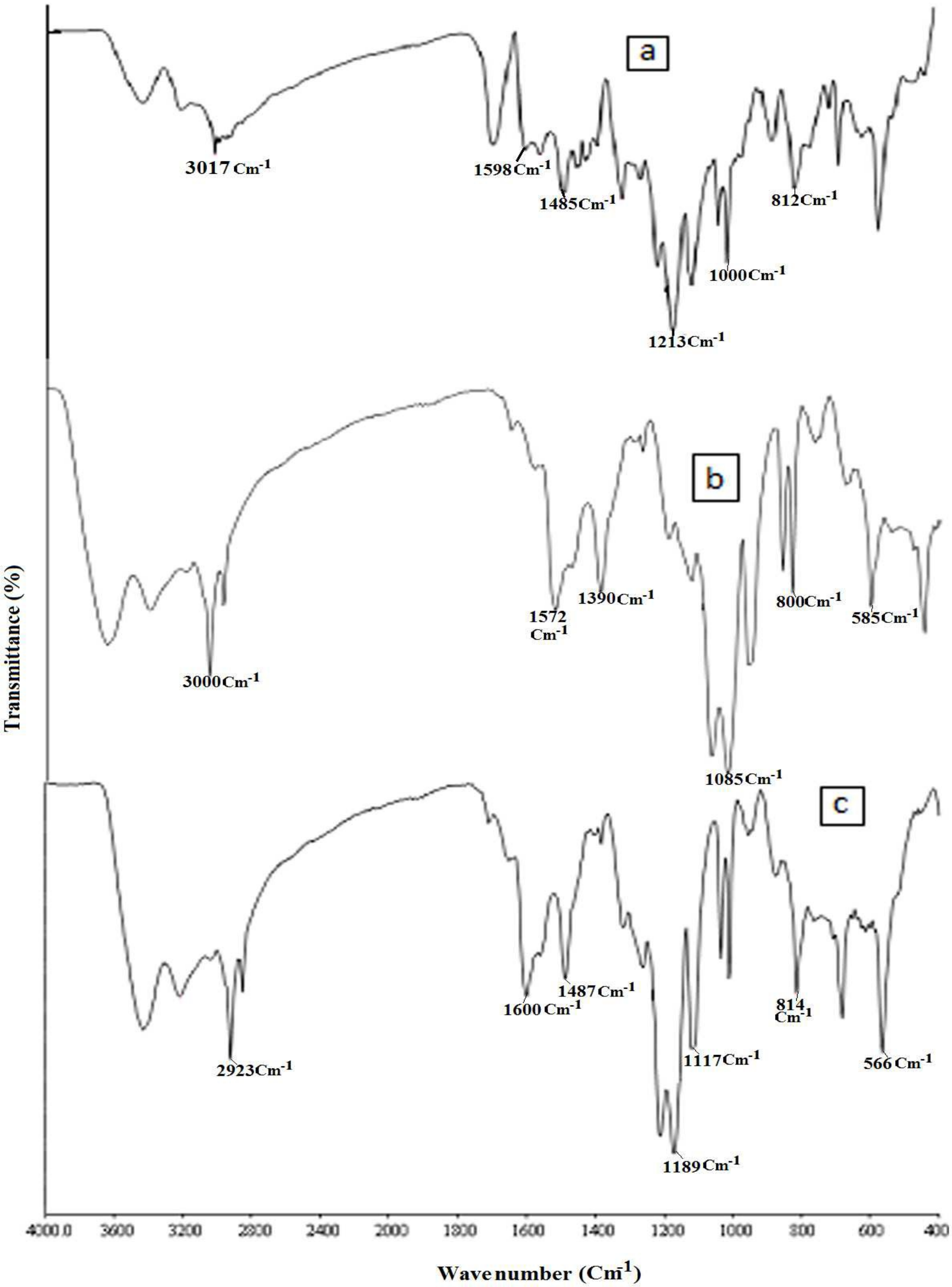

Figure 2. FTIR Spectra of (a) POT, (b) POT/MWCNTs and (c) POT/MWCNTs/ST composite ion exchanger

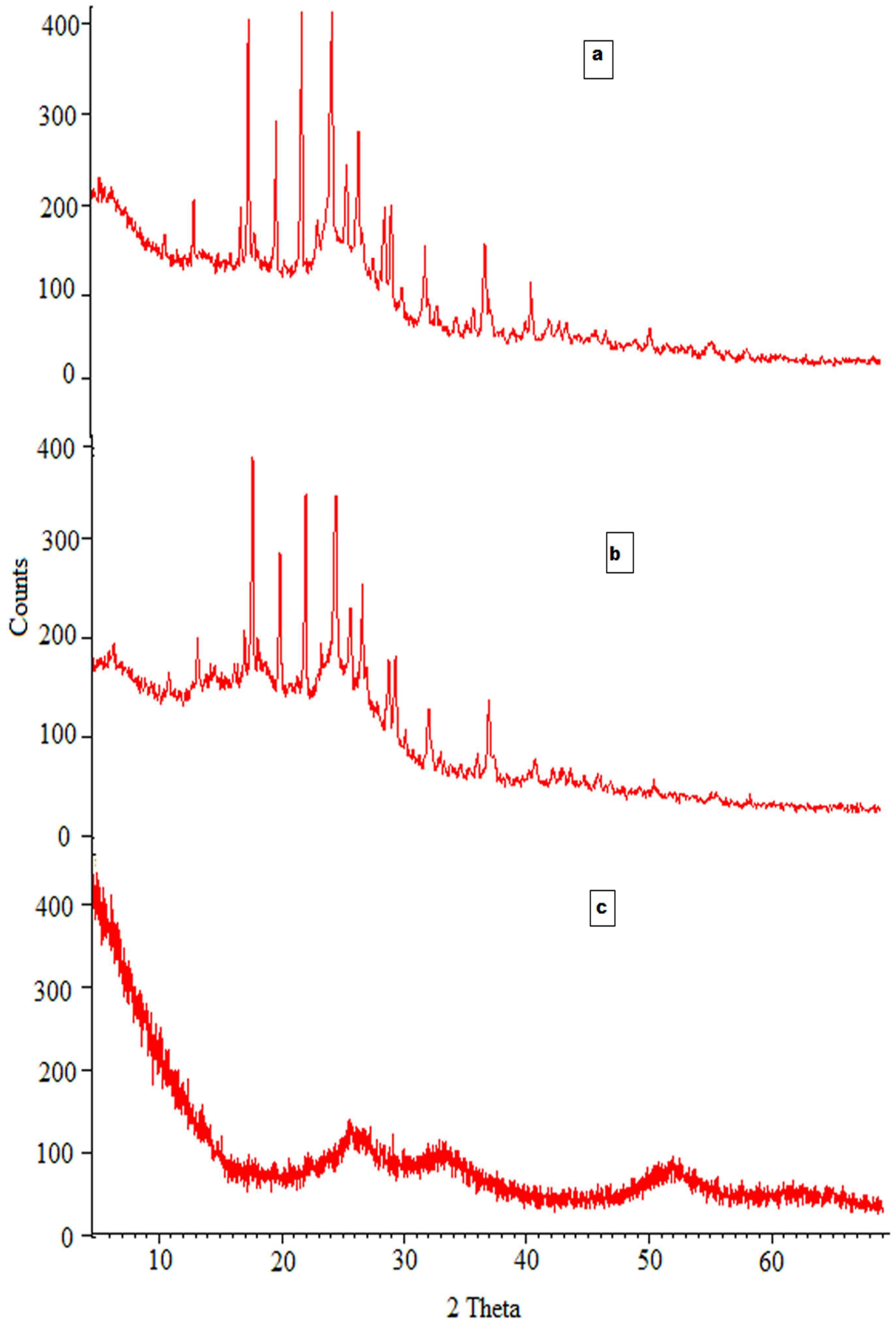

Figure 3. XRD pattern of (a) POT, (b) POT/MWCNTs and (c) POT/MWCNTs/ST composite ion exchanger

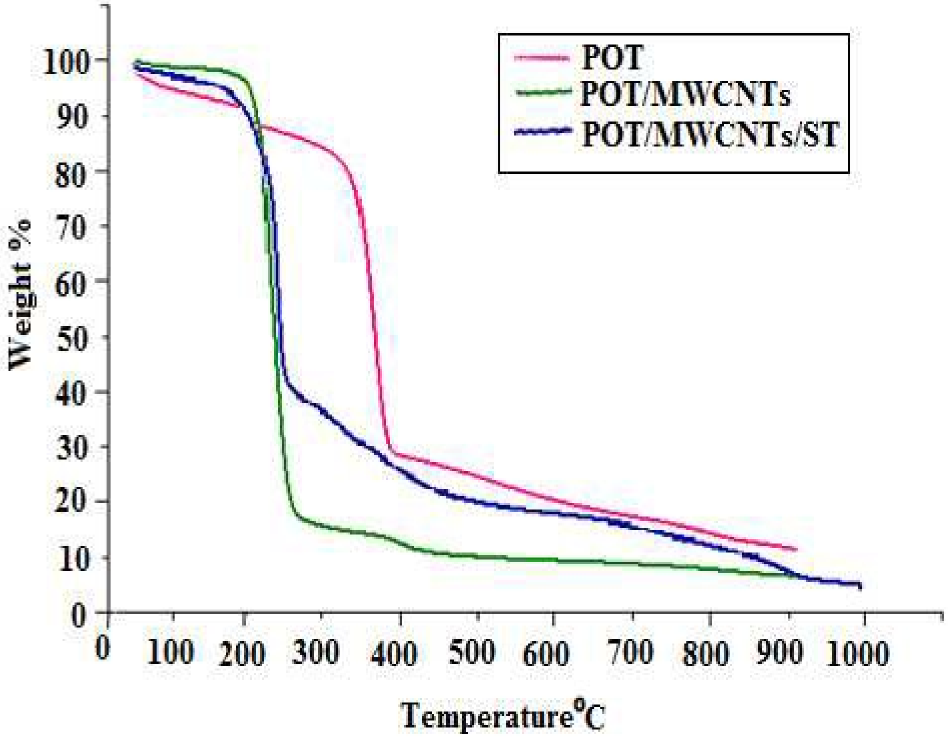

Figure 4. TGA curves of POT, POT/MWCNTs and POT/MWCNTs/ST composite ion exchanger

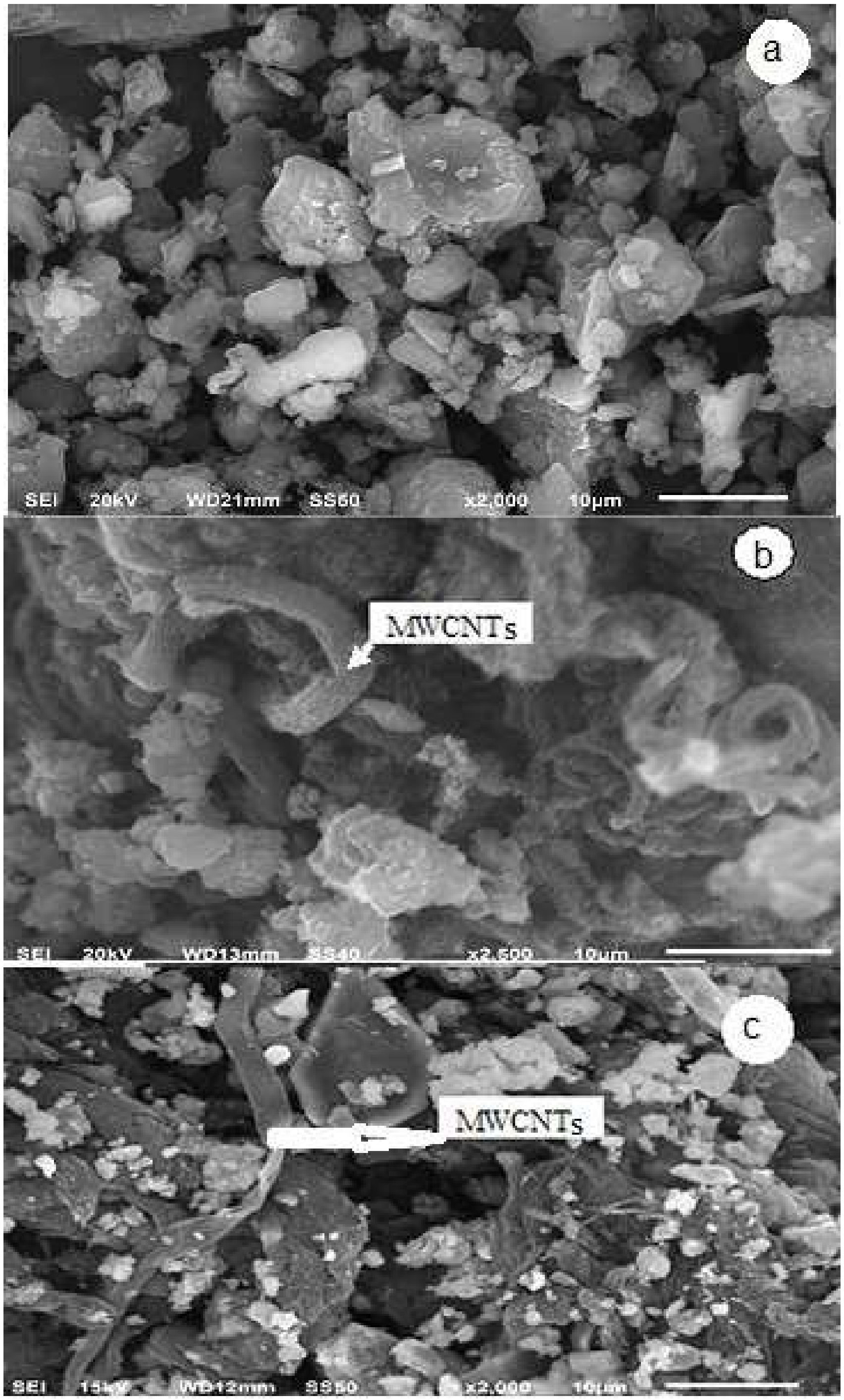

Figure 5. SEM photographs of (a) POT, (b) POT/MWCNTs and (c) POT/MWCNTs/ST composite ion exchanger

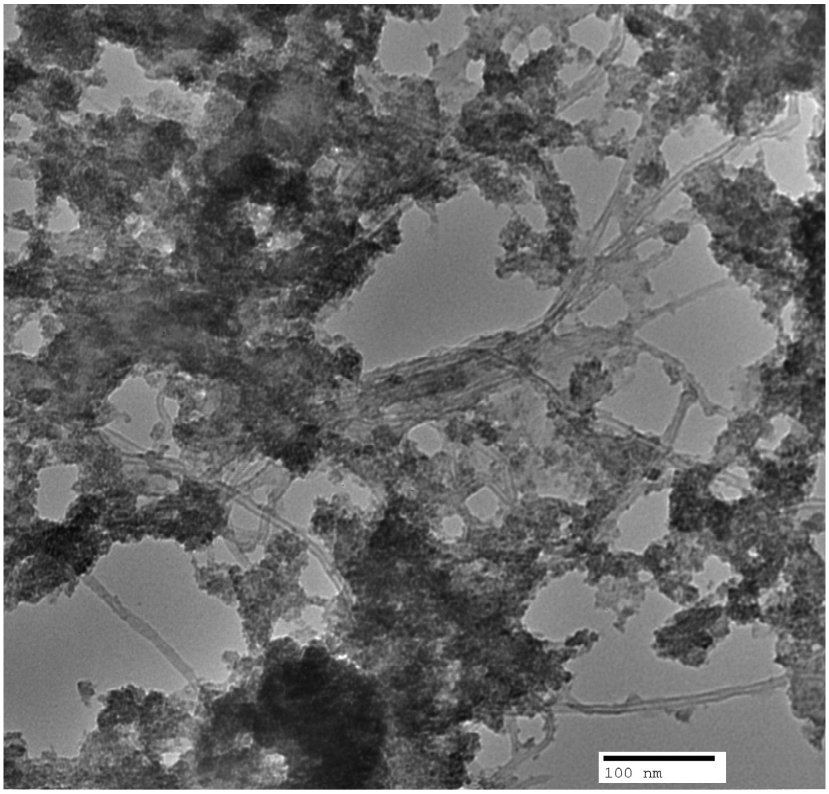

Figure 6. TEM micrographs of POT/MWCNTs/ST composite ion exchanger

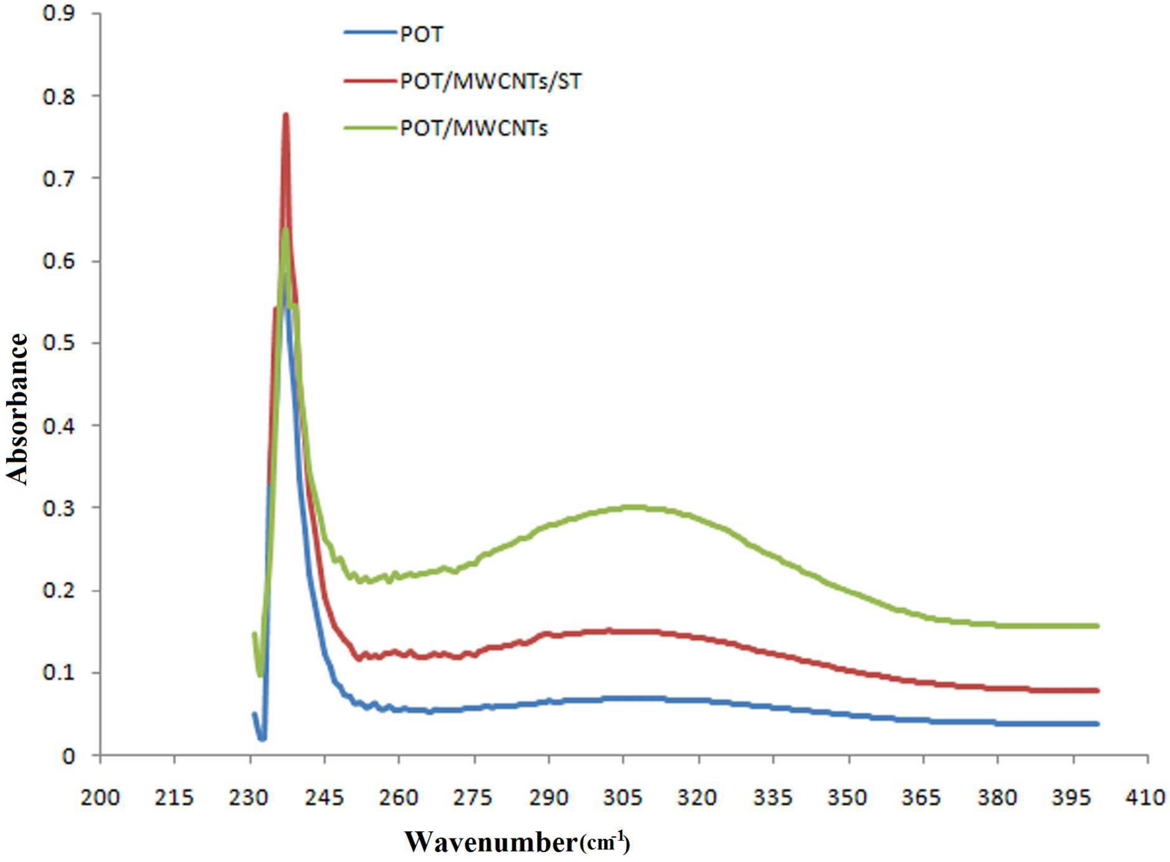

Figure 7. UV-Visible spectra of POT, POT/MWCNTs and POT/MWCNTs/ST composite ion exchanger

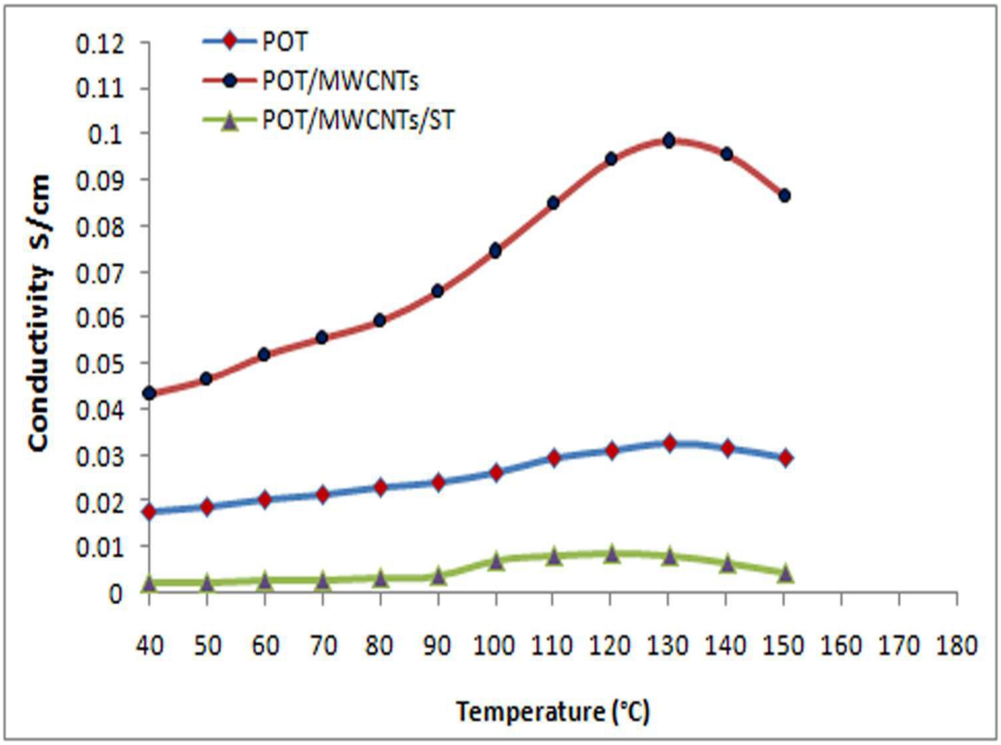

Figure 8. Conductivity of POT, POT/MWCNTs and POT/MWCNTs/ST composite ion exchanger at 40-150 °C temperature

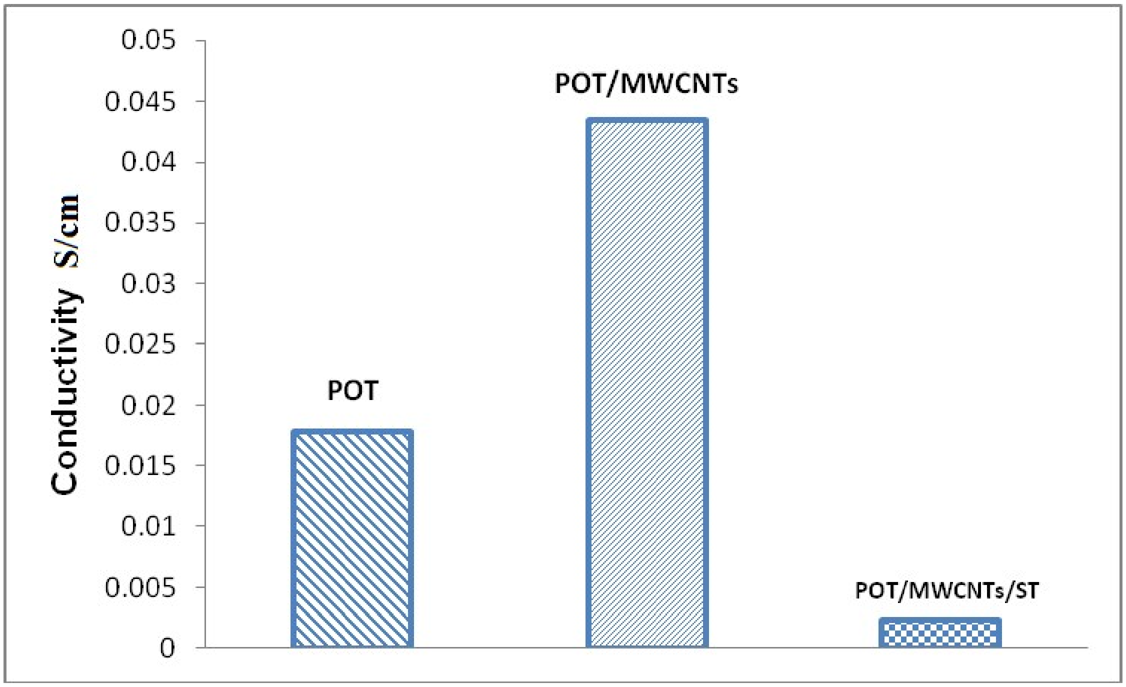

Figure 9. Initial conductivity of POT, POT/MWCNTs and POT/MWCNTs/ST composite ion exchanger

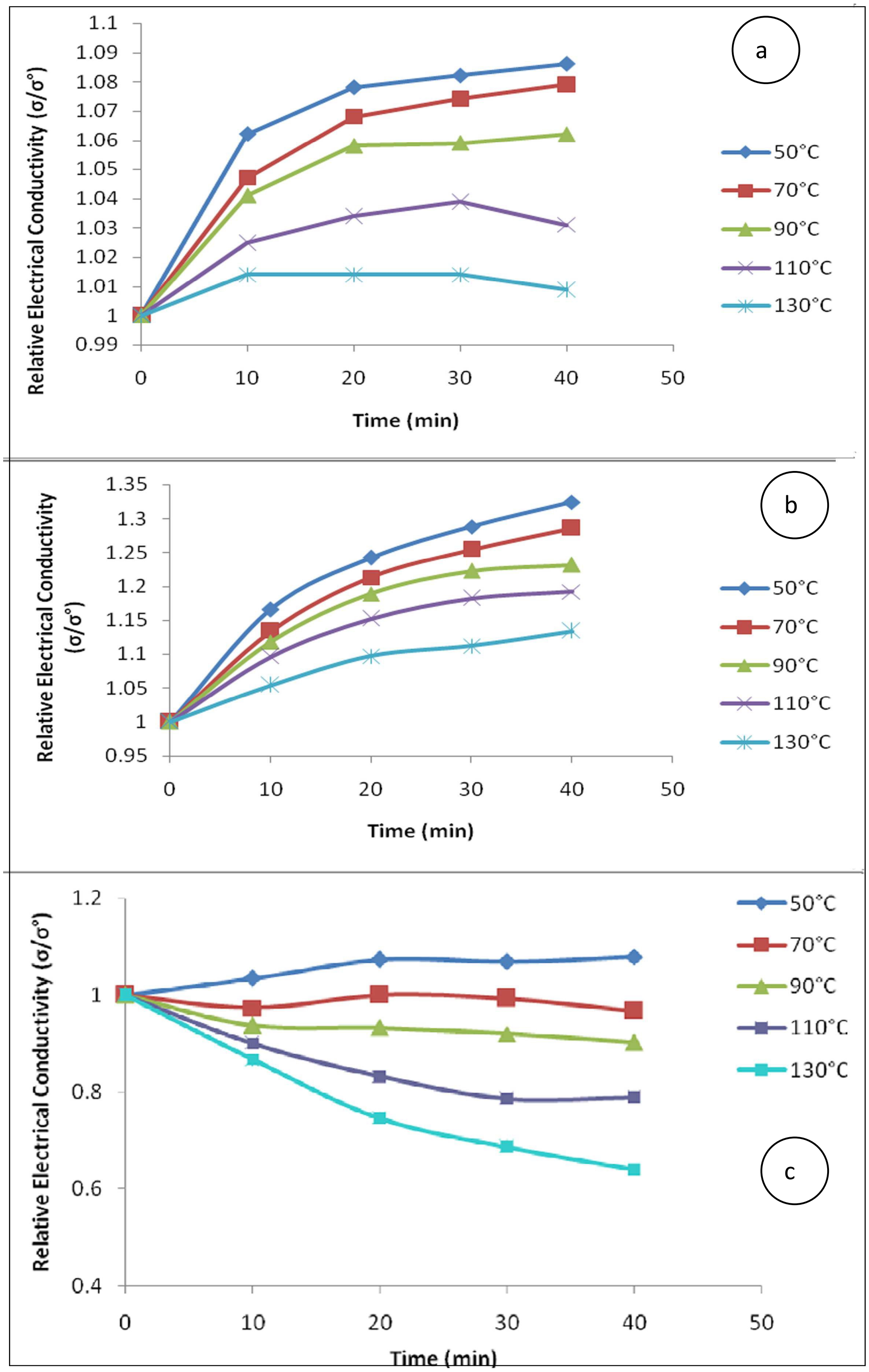

Figure 10. Isothermal Stability of (a) POT, (b) POT/MWCNTs and (c) POT/MWCNTs/ST composite ion exchangers in terms of D.C. electrical conductivity retention at 50,70, 90, 110 and 130 °C

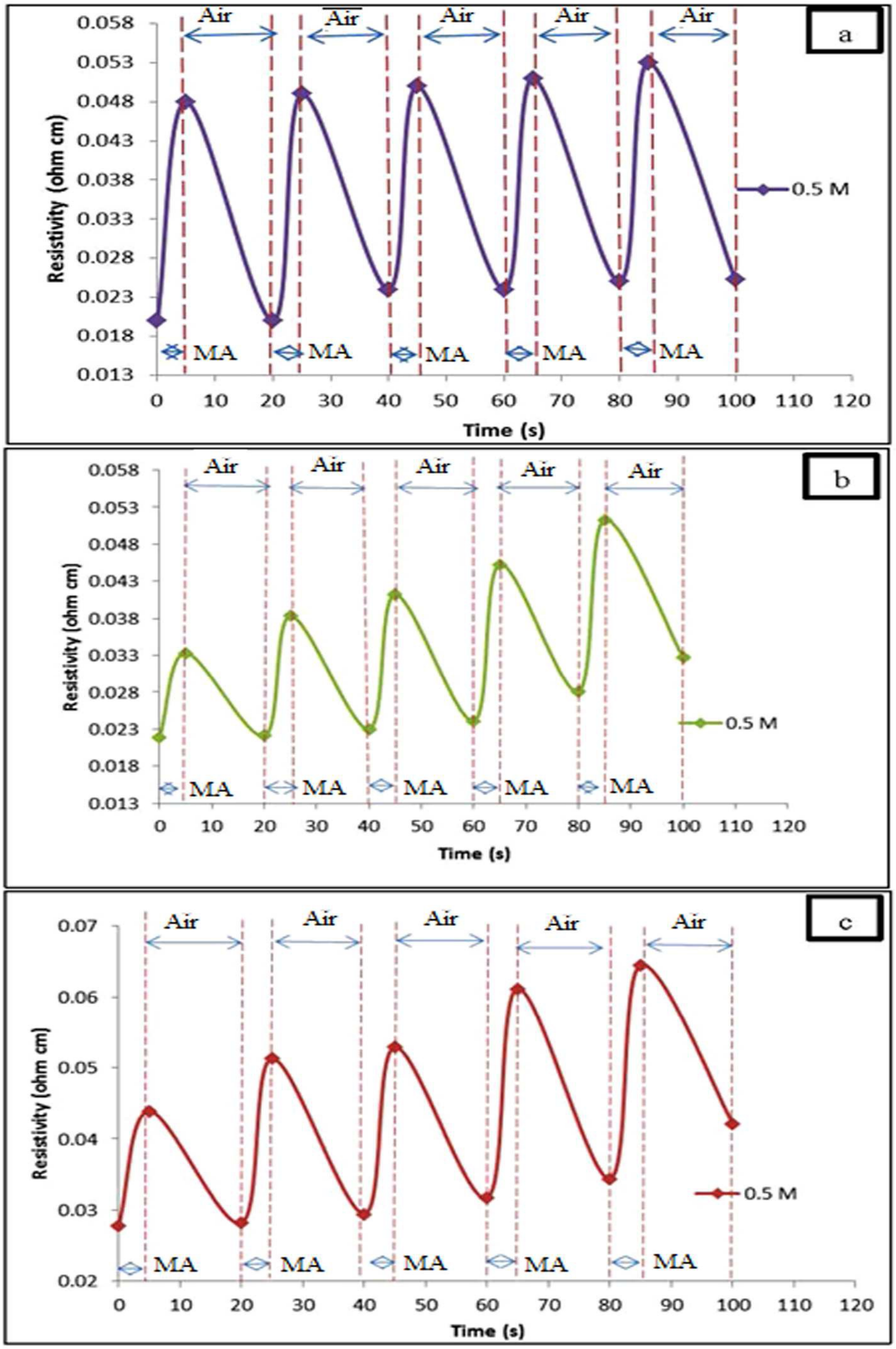

Figure 11(I). Variation in resistivity of *p*TSA doped (a)POT, (b)POT/MWCNTs and (c) POT/MWCNTs/ST composites ion exchanger on exposure to 0.5 M –CH_2NH_2 (MA)

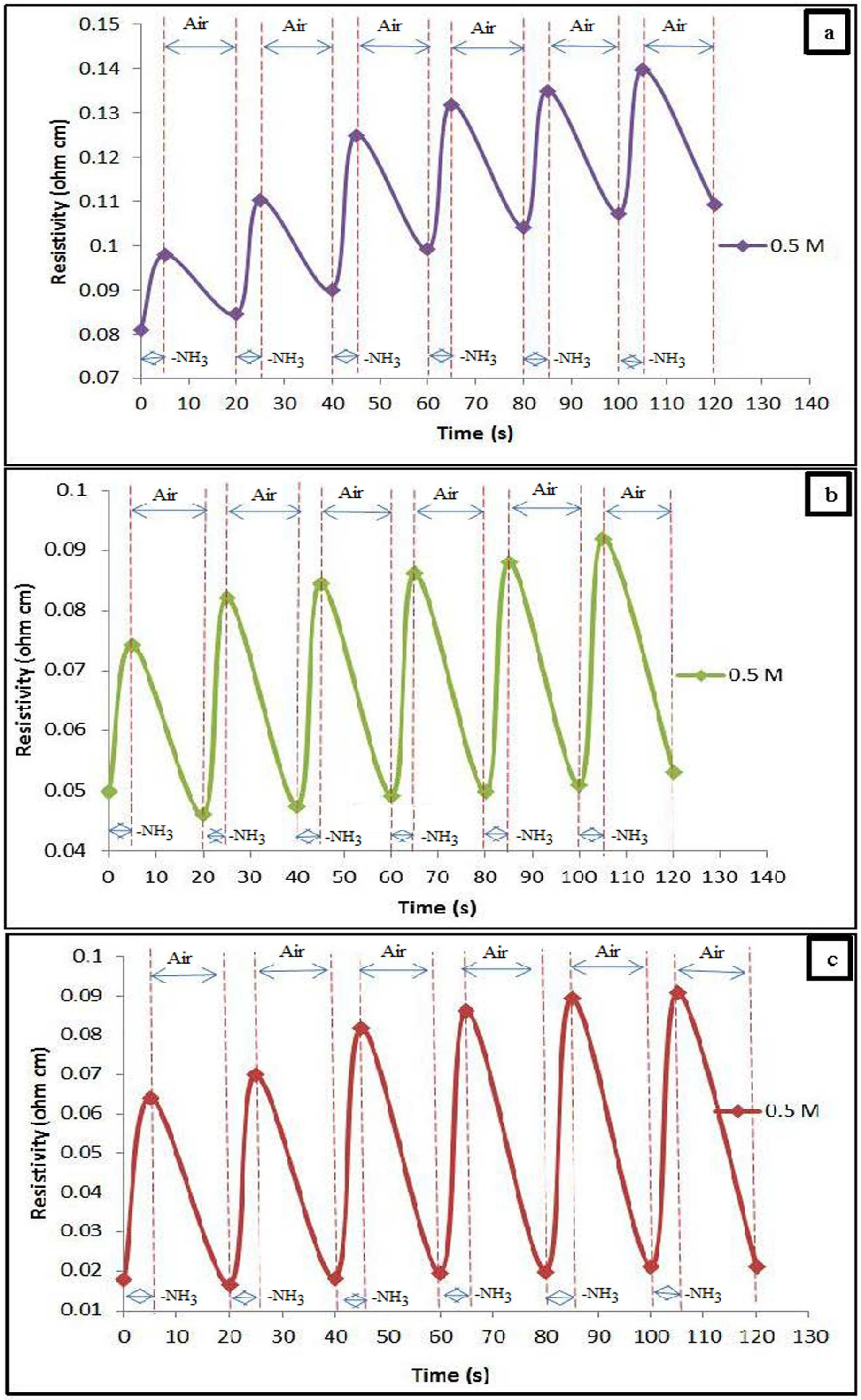

Figure 11(II). Variation in resistivity of *p*TSA doped (a)POT, (b)POT/MWCNTs and (c) POT/MWCNTs/ST composites ion exchanger on exposure to 0.5 M ammonia (NH_3)

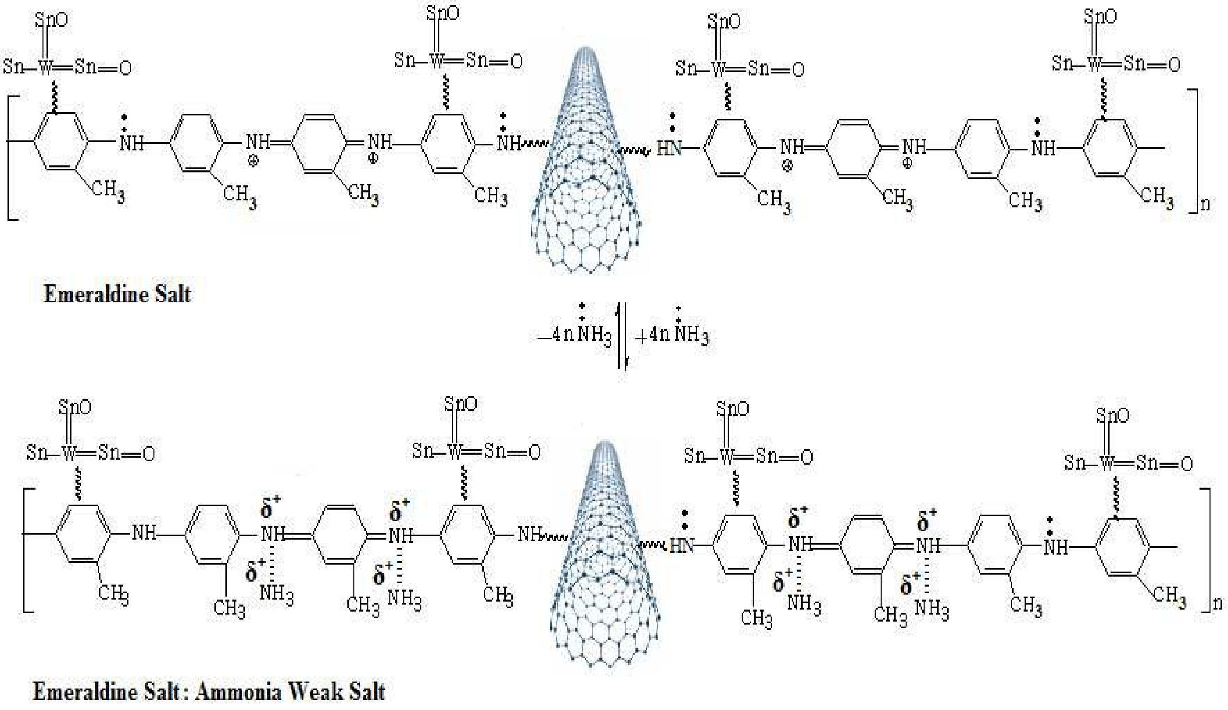

Scheme 2. The mechanistic representation of the electrical compensation of *p*TSA doped POT/MWCNTs/ST